REPORT DOCUMENTATION PAGE

Form Approved OMB NO. 0704-0188

1. REPORT DATE (DD-MM-YYYY)	2. REPORT TYPE	3. DATES COVERED (From - To)
12-10-2019	Final Report	15-Jul-2016 - 14-Jul-2019

4. TITLE AND SUBTITLE

Final Report: Robust Light State and Transport by Quantum Phase Transition in Non-Hermitian Photonic Materials

5a. CONTRACT NUMBER
W911NF-16-1-0403

5b. GRANT NUMBER

5c. PROGRAM ELEMENT NUMBER
611102

6. AUTHORS

5d. PROJECT NUMBER

5e. TASK NUMBER

5f. WORK UNIT NUMBER

7. PERFORMING ORGANIZATION NAMES AND ADDRESSES

State University of New York (SUNY) at Bu
The UB Commons
520 Lee Entrance, Suite 211
Amherst, NY 14228 -2567

8. PERFORMING ORGANIZATION REPORT NUMBER

9. SPONSORING/MONITORING AGENCY NAME(S) AND ADDRESS (ES)

U.S. Army Research Office
P.O. Box 12211
Research Triangle Park, NC 27709-2211

10. SPONSOR/MONITOR'S ACRONYM(S)
ARO

11. SPONSOR/MONITOR'S REPORT NUMBER(S)
68281-PH-YIP.9

12. DISTRIBUTION AVAILIBILITY STATEMENT

Approved for public release; distribution is unlimited.

13. SUPPLEMENTARY NOTES

The views, opinions and/or findings contained in this report are those of the author(s) and should not contrued as an official Department of the Army position, policy or decision, unless so designated by other documentation.

14. ABSTRACT

15. SUBJECT TERMS

16. SECURITY CLASSIFICATION OF:			17. LIMITATION OF ABSTRACT	15. NUMBER OF PAGES	19a. NAME OF RESPONSIBLE PERSON
a. REPORT	b. ABSTRACT	c. THIS PAGE			Liang Feng
UU	UU	UU	UU		19b. TELEPHONE NUMBER
					215-898-7106

Standard Form 298 (Rev 8/98)
Prescribed by ANSI Std. Z39.18

RPPR Final Report
as of 06-May-2020

Agency Code:

Proposal Number: 68281PHYIP **Agreement Number: W911NF-16-1-0403**

INVESTIGATOR(S):

Name: Liang Feng
Email: fenglia@seas.upenn.edu
Phone Number: 2158987106
Principal: Y

Organization: **State University of New York (SUNY) at Buffalo**
Address: The UB Commons, Amherst, NY 142282567
Country: USA
DUNS Number: 038633251 EIN: 141368361
Report Date: 14-Oct-2019 Date Received: 12-Oct-2019
Final Report for Period Beginning 15-Jul-2016 and Ending 14-Jul-2019
Title: Robust Light State and Transport by Quantum Phase Transition in Non-Hermitian Photonic Materials
Begin Performance Period: 15-Jul-2016 **End Performance Period:** 14-Jul-2019
Report Term: 0-Other
Submitted By: Liang Feng Email: fenglia@seas.upenn.edu
Phone: (215) 898-7106
Distribution Statement: 1-Approved for public release; distribution is unlimited.

STEM Degrees: 1 **STEM Participants:** 0

Major Goals: The objective of this project is to investigate fundamental phase transition properties of photonic materials with the foundation in quantum mechanics and mathematical physics, considering both non-Hermtian and topological symmetries, for unprecedented robust light manipulation.

The major goals are focused on the demonstration of novel interface light states enabled by quantum phase transition on the silicon-on-insulator and III-V semiconductor platforms. The project is conducted in 4 Thrusts:

Thrust I: An important objective is to construct theoretical models for novel topological photonic states. The related theoretical studies can be used to effectively characterize the related topological symmetries of the photonic structures and develop a structure of multiple quantum numbers. The quantum and topological phase transitions can be flexibly realized by switching the structure from one quantum number to the other.

Thrust II: Until now, a majority of experimentally and theoretically studied non-Hermitian photonic materials were based on single-phase photonic structures, in either symmetric or broken PT, but not on both. In other words, the unique genus of quantum phase invariant with respect to phase transitions has not been effectively utilized and explored. In this project, we have demonstrated the non-Hermitian topological light state and better understand how the interface state emerges as a function of non-Hermiticity.

Thrust III: One important characteristic of the demonstrated topological interface state is that it is protected by the particle-hole symmetry, producing a robust photonic zero mode. It is therefore important to verify the robustness of the interface light state against topological defects and investigate the robust transport characteristics of this interface state. Potential advantages include fault-tolerant light transport against a variety of impurities, defects, and structural disorders.

Thrust IV: Another particular interest on non-Hermitian photonic materials is to strategically utilize optical non-Hermiticity to design the interplay between gain and loss in laser cavities, enabling ultrastable lasing emission immune to a variety of environmental variations. By exploiting the robust light state, ultrastable lasing radiation can be envisioned with a high amplification rate and elimination of undesired mode hopping. The associated dynamics of the light-matter interaction and emission control by the robust light state can be experimentally studied.

Accomplishments: In this project, we have successfully advanced the fundamental relation of topological symmetries and their couplings with non-Hermitian symmetries, which enriched topological physics and delivered novel topological photonic states. According to the 4 proposed research thrusts, we have theoretically and experimentally accomplished: 1) Photonic lattices of multiple topological quantum numbers; 2) Non-Hermitian-induced robust topological photonic states, and 3) Topological microring laser arrays.

Please see the uploaded PDF file for details.

Training Opportunities: Nothing to Report

Results Dissemination: Throughout the project period, we have published 8 manuscripts, including 1 in Nature Photonics, 3 in Nature Communications, 1 in National Science Review, 1 in Laser & Photonics Reviews, 1 in PRA and 1 in PRB.

Honors and Awards: PI Liang Feng was elected to the fellow of the Optical Society of America (OSA) in October 2018 and received the Young Scientist Award from Microsystems and Nanoengineering in 2018, and the OSA Best Young Research Prize presented during CLEO Pacific Rim in 2017.

Protocol Activity Status:

Technology Transfer: Nothing to Report

PARTICIPANTS:

Participant Type: PD/PI
Participant: Liang Feng
Person Months Worked: 3.00 **Funding Support:**
Project Contribution:
International Collaboration:
International Travel:
National Academy Member: N
Other Collaborators:

Participant Type: Graduate Student (research assistant)
Participant: Pei Miao
Person Months Worked: 6.00 **Funding Support:**
Project Contribution:
International Collaboration:
International Travel:
National Academy Member: N
Other Collaborators:

Participant Type: Graduate Student (research assistant)
Participant: Mingsen Pan
Person Months Worked: 10.00 **Funding Support:**
Project Contribution:
International Collaboration:
International Travel:
National Academy Member: N
Other Collaborators:

ARTICLES:

Publication Type: Journal Article Peer Reviewed: Y **Publication Status:** 1-Published
Journal: Physical Review B
Publication Identifier Type: DOI Publication Identifier: 10.1103/PhysRevB.95.165109
Volume: 95 Issue: First Page #: 165109
Date Submitted: 8/30/17 12:00AM Date Published:
Publication Location:
Article Title: Topological tight-binding models from nontrivial square roots
Authors: J. Arkinstall, M. H. Teimourpour, L. Feng, R. El-Ganainy, and H. Schomerus
Keywords: Topological symmetry, Quantum number
Abstract: We describe a versatile mechanism that provides tight-binding models with an enriched, topologically nontrivial band structure. The mechanism is algebraic in nature, and leads to tight-binding models that can be interpreted as a nontrivial square root of a parent lattice Hamiltonian-in analogy to the passage from a Klein-Gordon equation to a Dirac equation. In the tight-binding setting, the square-root operation admits to induce spectral symmetries at the expense of broken crystal symmetries. As we illustrate in detail for a simple one-dimensional example, the emergent and inherited spectral symmetries equip the energy gaps with independent topological quantum numbers that control the formation of topologically protected states. We also describe an implementation of this system in silicon photonic structures, outline applications in higher dimensions, and provide a general argument for the origin and nature of the emergent symmetries, which are typically nonsymmorphic.
Distribution Statement: 3-Distribution authorized to U.S. Government Agencies and their contractors
Acknowledged Federal Support: **Y**

Publication Type: Journal Article Peer Reviewed: Y **Publication Status:** 1-Published
Journal: Nature Photonics
Publication Identifier Type: Publication Identifier:
Volume: 11 Issue: First Page #: 752
Date Submitted: 8/29/18 12:00AM Date Published: 11/30/17 10:00AM
Publication Location:
Article Title: Non-Hermitian Photonics Based on Parity-Time Symmetry
Authors: Liang Feng, Ramy El-Ganainy, Li Ge
Keywords: non-Hermitian photonic, parity-time symmetry
Abstract: Nearly one century after the birth of quantum mechanics, parity-time (PT) symmetry is revolutionizing and extending quantum theories to include a unique family of non-Hermitian Hamiltonians. While conceptually striking, experimental demonstration of PT symmetry remains unexplored in quantum electronic systems. Although photonics generally has different focuses, its flexibility allows for creating and superposing non-Hermitian eigenstates with ease using optical gain and loss, which makes it an ideal platform to explore various non-Hermitian quantum symmetry paradigms for novel device functionalities. These explorations on classical photonic platforms not only deepen our understanding of fundamental quantum physics but also facilitate technological breakthroughs for photonics applications. Hence, researches in non-Hermitian photonics of such two-fold benefits are advancing both fields simultaneously.
Distribution Statement: 3-Distribution authorized to U.S. Government Agencies and their contractors
Acknowledged Federal Support: **Y**

Publication Type: Journal Article Peer Reviewed: Y **Publication Status:** 1-Published
Journal: Nature Communications
Publication Identifier Type: DOI Publication Identifier: 10.1038/s41467-018-03434-2
Volume: 9 Issue: 1 First Page #:
Date Submitted: 8/29/18 12:00AM Date Published: 3/1/18 12:00AM
Publication Location:
Article Title: Topological hybrid silicon microlasers
Authors: Han Zhao, Pei Miao, Mohammad H. Teimourpour, Simon Malzard, Ramy El-Ganainy, Henning Schome
Keywords: non-Hermitian, topological, microlaser
Abstract: Topological physics provides a robust framework for strategically controlling wave confinement and propagation dynamics. Active systems provide a more general framework where different fundamental symmetry paradigms, such as those arising from non-Hermiticity and nonlinear interaction, can generate a new landscape for topological physics and its applications. Here, we bridge this gap and present an experimental investigation of an active topological photonic system, demonstrating a topological hybrid silicon microlaser array respecting the charge-conjugation symmetry. The created new symmetry features favour the lasing of a protected zero mode, where robust single-mode laser action in the desired state prevails even with intentionally introduced perturbations. The demonstrated microlaser is hybrid implemented on a silicon-on-insulator substrate, and is hybrid implemented on a silicon-on-insulatorsubstrate.
Distribution Statement: 3-Distribution authorized to U.S. Government Agencies and their contractors
Acknowledged Federal Support: **Y**

Publication Type: Journal Article Peer Reviewed: Y **Publication Status:** 1-Published
Journal: Nature Communications
Publication Identifier Type: DOI Publication Identifier: 10.1038/s41467-018-03822-8
Volume: 9 Issue: 1 First Page #:
Date Submitted: 8/29/18 12:00AM Date Published: 4/1/18 12:00AM
Publication Location:
Article Title: Photonic zero mode in a non-Hermitian photonic lattice
Authors: Mingsen Pan, Han Zhao, Pei Miao, Stefano Longhi, Liang Feng
Keywords: zero mode, non-Hermitian, phase transition
Abstract: Here we demonstrate a robust photonic zero mode sustained by a spatial non-Hermitian phase transition in a parity-time (PT) symmetric lattice, despite the same topological order across the entire system. The non-Hermitian-enhanced topological protection ensures the reemergence of the zero mode at the phase transition interface when the two semi-lattices under different PT phases are decoupled effectively in their real spectra. Residing at the midgap level of the PT symmetric spectrum, the zero mode is topologically protected against topological disorder. We experimentally validated the robustness of the zero-energy mode by ultrafast heterodyne measurements of light transport dynamics in a silicon waveguide lattice.
Distribution Statement: 3-Distribution authorized to U.S. Government Agencies and their contractors
Acknowledged Federal Support: **Y**

Publication Type: Journal Article Peer Reviewed: N **Publication Status:** 1-Published
Journal: Nature Communications
Publication Identifier Type: DOI Publication Identifier: 10.1038/s41467-018-05175-8
Volume: 9 Issue: 1 First Page #:
Date Submitted: 8/29/18 12:00AM Date Published: 7/1/18 4:00AM
Publication Location:
Article Title: Non-Hermitian photonics promises exceptional topology of light
Authors: Bikashkali Midya, Han Zhao, Liang Feng
Keywords: non-Hermitian photonics, exceptional point, topology
Abstract: The band degeneracy, either the exceptional point of a non-Hermitian system or the Dirac point associated with a topological system, can feature distinct symmetry and topology. Their synergy will further produce more exotic topological effects in synthetic matter.
Distribution Statement: 3-Distribution authorized to U.S. Government Agencies and their contractors
Acknowledged Federal Support: **Y**

RPPR Final Report
as of 06-May-2020

Publication Type: Journal Article Peer Reviewed: Y **Publication Status:** 1-Published
Journal: National Science Review
Publication Identifier Type: DOI Publication Identifier: 10.1093/nsr/nwy011
Volume: 5 Issue: 2 First Page #: 183
Date Submitted: 8/29/18 12:00AM Date Published: 3/1/18 5:00AM
Publication Location:
Article Title: Parity–time symmetric photonics
Authors: Han Zhao, Liang Feng
Keywords: photonics, parity–time symmetry, non-Hermitian, phase transition, exceptional point
Abstract: The establishment of non-Hermitian quantum mechanics (such as parity–time (PT) symmetry) stimulates a paradigmatic shift for studying symmetries of complex potentials. Owing to the convenient manipulation of optical gain and loss in analogy to complex quantum potentials, photonics provides an ideal platform for the visualization of many conceptually striking predictions from non-Hermitian quantum theory. A rapidly developing field has emerged, namely, PT-symmetric photonics, demonstrating intriguing optical phenomena including eigenstate coalescence and spontaneous PT-symmetry breaking. The advance of quantum physics, as the feedback, provides photonics with brand-new paradigms to explore the entire complex permittivity plane for novel optical functionalities. Here, we review recent exciting breakthroughs in PT-symmetric photonics while systematically presenting their underlying principles guided by-Hermitian symmetries. The potential device applications for optical communication an
Distribution Statement: 3-Distribution authorized to U.S. Government Agencies and their contractors
Acknowledged Federal Support: **Y**

Publication Type: Journal Article Peer Reviewed: Y **Publication Status:** 1-Published
Journal: Physical Review A
Publication Identifier Type: DOI Publication Identifier: 10.1103/PhysRevA.98.043838
Volume: 98 Issue: First Page #: 043838
Date Submitted: 10/11/19 12:00AM Date Published: 10/19/18 8:00AM
Publication Location:
Article Title: Topological multiband photonic superlattices
Authors: Bikashkali Midya, Liang Feng
Keywords: Topological superlattice, multiband topology
Abstract: A one-dimensional discrete lattice of dimers is known to possess topologically protected edge states when interdimer coupling is stronger than intradimer coupling. Here, we address richer topological properties of photonic superlattices having an arbitrary number of elements in each unit cell. It is shown that the superlattice provides a tunable number of topologically protected edge and interface states depending on certain restrictions on intra-and intercell couplings maintaining inversion symmetry of the lattice. Simultaneous and stable propagation of multiple topological interface states, their interference pattern, and stable oscillation are reported. The configuration can be relevant for topologically protected mode-division multiplexing through a narrow route in photonic devices.
Distribution Statement: 1-Approved for public release; distribution is unlimited.
Acknowledged Federal Support: **Y**

RPPR Final Report
as of 06-May-2020

Publication Type: Journal Article Peer Reviewed: Y **Publication Status:** 1-Published
Journal: Laser & Photonics Reviews
Publication Identifier Type: DOI Publication Identifier: 10.1002/lpor.201800202
Volume: 13 Issue: First Page #: 1800202
Date Submitted: 10/11/19 12:00AM Date Published: 1/3/19 5:00AM
Publication Location:
Article Title: Experimental Realization of Multiple Topological Edge States in a 1D Photonic Lattice
Authors: Zhifeng Zhang, MohammadTeimourpour, Jake Arkinstall, Mingsen Pan, Pei Miao, Henning Schomerus,
Keywords: Multiband topological edge states
Abstract: Topological photonic systems, such as the Su–Schrieffer–Heeger and Rice–Mele models, support only a limited number of nontrivial phases due to restrictions on dispersion band engineering. Here, a flexible topological photonic lattice on a silicon photonic platform is experimentally demonstrated that realizes multiple topologically nontrivial dispersion bands. By suitably setting the couplings between the 1D waveguides, different lattices can exhibit the transition between multiple different topological phases and allow the independent realization of the corresponding edge states. Heterodyne measurements clearly reveal the ultrafast transport dynamics of the edge states in different phases at a femtosecond scale, validating the designed topological features. The study equips topological models with enriched edge dynamics and considerably expands the scope to engineer unique topological features into photonic, acoustic, and atomic systems.
Distribution Statement: 1-Approved for public release; distribution is unlimited.
Acknowledged Federal Support: **Y**

Photonic Lattices of Multiband Topology

Topology, which originates from mathematics and deals with quantities that preserve their values during any continuous deformation, has firmly emerged as a new paradigm for describing new phases of matter since its first applications to condensed matter systems over three decades ago. To date, the SSH Hamiltonian serves as an archetypical model for describing topological physics and designing practical structures. However, the topological features of this conventional model are limited to only two dispersion bands, thereby permitting only a limited range of quantum numbers and consequently restricting the accessible nontrivial phases. Much can be gained from richer models with a large range of nontrivial phases that can be manipulated systematically to control the formation of independent topological states. Here, we demonstrate the formation and control of topological edge states associated with multiple topological quantum numbers in a discrete photonic lattice.

Our studies have delivered a topological photonic superlattice that can support multiple independent topological states. Instead of the simple dimer model in the classical SSH model, our Dirac procedure after iterations leads to a multicomponent unit cell (the number of sites in each unit cell is J) where the neighboring couplings between two adjacent components are strategically distributed (**Fig. 1a**), corresponding to a 1D multiband system where multiple topological states are found in different band gaps (**Fig. 1**). In this case, the spectrum of the system appears in two distinct forms: spectrum with (**Fig. 1c, e, g**) /without (**Fig. 1b, d, f**) topological states inside all the $(J-1)$ energy gaps when the intercell coupling τ is greater (less) than intracell couplings. Note that different topological states feature multiple quantum numbers.

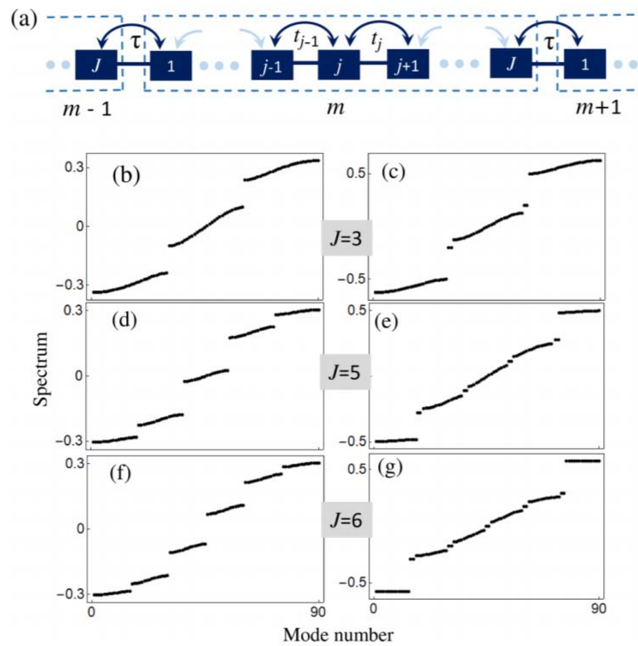

Figure 1. Multiband superlattices. (a) A schematic of a photonic superlattice with J elements in each unit cell. t_j and τ are intracell and intercell couplings, respectively. (b)–(g) Eigenspectrum β of superlattices with (b),(c) J = 3, (d),(e) J = 5, and (f),(g) J = 6 elements in a unit cell. The emergence of bound states inside the energy gap is seen in (c), (e), and (g), if the intercell and intracell couplings are properly designed. [16]

We have further designed a photonic waveguide lattice that can feature such multiband topology and experimentally verified the phase transition from one topological quantum number to another., The multiband topological lattice (**Fig. 2a**) provides controls to design different Bloch eigenstates formed through hybridizations of the supermodes associated with the dimers/waveguides. As shown in **Fig. 2b**, with the nonvanishing detuning $\Delta\beta$ of the propagation constants between the large and small waveguide in each of the dimer, the supermodes are highly localized in the large (base) or small (vertex) waveguides. Two supermodes each are close to resonance, experiencing effective coupling strengths alternating between strong and weak. This effect can be viewed as two SSH Hamiltonians (SSH $_I$ and SSH $_{II}$) occupying the same space yet having independent topological quantum numbers. As each SSH model creates two eigenvalues $\lambda_{\pm}$, the designed bowtie lattice is expected to demonstrate four dispersion bands, which is indeed borne out by direct modelling [**Fig. 2c**]. The coupling strengths and propogation constants are engineered to demonstrate different topological phases and thus control the related edge states. In the top panel of Fig. 1(c), the design parameters were chosen to be $\tilde{\kappa} = 1$, $\kappa = 0.5$ and $\beta_1 = -\beta_2 = 1$. As expected from the previous discussion, the system resembles two separate SSH Hamiltonians giving rise to two upper (SSH $_I$) and two lower (SSH $_{II}$) bands. The two isolated eigenvalues in the spectrum (one in the upper and another in the lower band gaps) correspond to states localized at the left and right edge state. This is in contrast to the conventional SSH model, for which the two edge states would lie in the same gap. The middle and lower panels of Fig. 1(c) highlight a crucial additional feature of this model—the existence of a third, central gap that separates the two effective SSH models. The design parameters are the same as used in the top panel, but for $\kappa = \sqrt{2}$ and 2, respectively. The central gap closes at $\kappa = \sqrt{2}$ while in the lower panel the gap is again opened. This band inversion gives rise to an additional pair of isolated eigenvalues, which are accompanied by the emergence of two new edge states. These edge states are associated with the spectral symmetry of the bowtie chain, which induces an additional topological quantum number - a feature that can be understood by inspecting the Zak phase and Witten index associated with each bulk band and each bandgap, respectively. In a continuum approximation, the two low-energy solutions at $k = 0$ give rise to two slowly varying fields that can be grouped into a spinor φ. Its evolution takes the form of a Jackiw-Rebbi model $id\varphi/dz = H_{\mathrm{eff}}\varphi$ with an effective Hamiltonian $H_{\mathrm{eff}} = m\sigma_z + v_F\sigma_y\hat{p}_x$, again in complete analogy with the SSH model. All three effective models are therefore associated with a chiral symmetry $\sigma_x H_{eff}\sigma_x = -H_{eff}$ guaranteeing topological physics in each gap. By controlling the inter-dimer and intra-dimer coupling strengths in the designed bowtie photonic lattice, we are able to independently switch the topological phases of these three coexisting models and can control the corresponding edge states on demand.

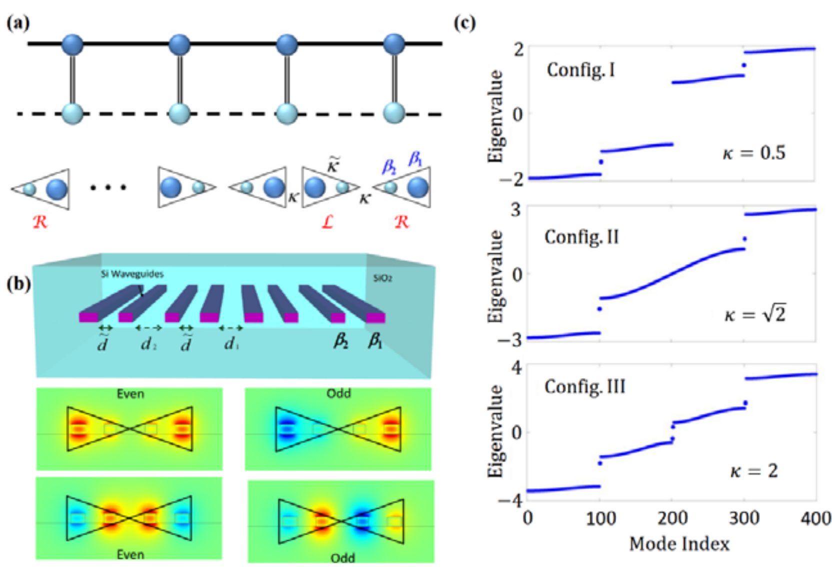

Figure 2. Bowtie topological lattice supporting two quantum numbers. (a) Two-legged ladder model having identical sites (top panel). Single and double lines represent couplings of different strength; the dashed lines signify couplings of opposite sign from the solid lines. Taking the square root and a Z_2 gauge transformation of this model results in the bowtie chain shown in the lower panel, with alternating couplings κ, $\tilde{\kappa}$ and staggered sequence of onsite energies $\beta_1, \beta_2, \beta_2, \beta_1$, ... As indicated, this can be interpreted as a sequence of oppositely orientated dimers, labelled by L and R. (b) Implementation of the bowtie lattice using silicon waveguides embedded in silica cladding. (c) Band structures of bowtie arrays with $\tilde{\kappa} = 1$, $\beta_1 = -\beta_2 = 1$ and different values of κ.

For the experiments, we fabricated three different samples of the photonic lattice with controlled physical parameters corresponding to different configurations I, II and III as defined in **Fig. 2c.** On an SOI platform, each sample consisted of 18 guiding channels. The scanning electron microscope pictures corresponding to configuration III are shown in **Fig. 3**.

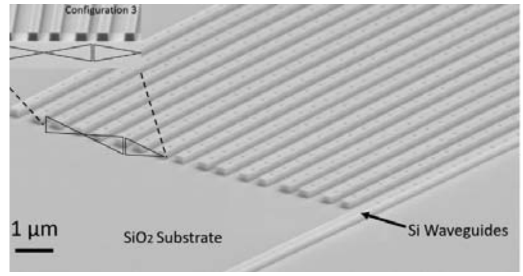

Figure 3. Scanning electron microscope pictures of the device (configuration III)

We applied the time-resolved spatial-heterodyne imaging technique, which provides the spatial distribution of the light versus time. Thus, we could characterize the ultrafast transport dynamics in the observed edge states (**Fig. 4**). These ultrafast temporal measurements provide access to quantitative characteristics of the edge state.

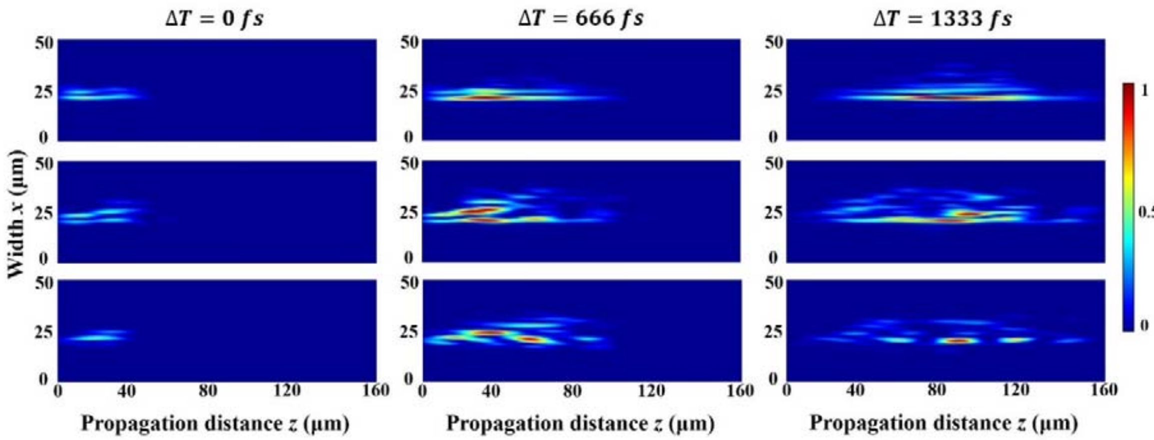

Figure 4. Measured ultrafast transport dynamics in the bowtie topological waveguide lattices. Temporal evolution of spatial intensity of the wave packet is captured with a time delay of ~66.6 fs for configurations I, II and III (top, middle, and bottom panels, respectively). Images are normalized with the same input power, assuming a lossless propagation in the z direction. Field intensity spatial maps in left, middle, and right colums correspond to different time delays at $\Delta T = 0, 666,$ and 1333 fs, respectively, showing the wave packet entering the lattice, the formation of the edge states at the beginning of the lattice, and the transport of the edge states in the lattice.

All the edge states are associated with distinct dynamical properties encoded in the effective group and phase indices, which provide additional quantitative assessments of each state. In configuration I, the group index $n_g = 3.30 \pm 0.012$ (calculation details can be found in supporting information) can be retrieved through pulse positions traveled at different time delays, corresponding to an effective index of $n_{eff} = 1.67 \pm 0.012$ that agrees well with the simulation $n_{eff} = 1.72$. For configuration II, it is clearly demonstrated that the dynamical transport of the single edge state is accompanied by a secondary emission, revealing the closure of the central bandgap. Their interference, while weak, slightly distorts the field distribution and the propagation of the wave packet in the launching channel. The measured group index is consistently lower than configuration I, $n_g = 3.23 \pm 0.011$ with $n_{eff} = 1.66 \pm 0.011$. For configuration III, the dynamical evolution of the wave packet is revealed by the interference beating due to the co-propagation of two topological edge states with distinct propagation constants measured group index $n_g = 3.18 \pm 0.015$ in this case is the averaged group index of the two edge states. Their respective effective indices are $n_{eff,1} = 1.70 \pm 0.015$ and $n_{eff,2} = 1.65 \pm 0.015$. In contrast, a uniformly arranged trivial waveguide array shows a diffraction pattern corresponding to free spreading and reflection of the wave packet across the whole array. This is distinct from the topological edge modes observed in the previous 3 configurations.

In summary, with the multiband topological model, we designed and experimentally demonstrated a versatile photonic lattice with multi-band topology. Compared with the conventional Su-Schrieffer Heeger and Rice-Mele models, the lattice offers additional spectral symmetries that enrich the topological features and enable to induce independently tuned edge states. We experimentally investigated the ultrafast beam transport dynamics to validate the supported topological characteristics. Through systematically manipulating the couplings in the lattice, the topological nature of multiple dispersion bands can be effectively engineered with a desired Witten index in different energy bandgaps, enabling the versatile realization of topologically-induced edge state dynamics.

Novel Non-Hermitian-Governed Topological Interface State

Topological zero states are expected play an important role in fault-tolerant quantum computation. In conventional Hermitian quantum systems, however, such zero states are vulnerable and even become vanishing if couplings with surroundings are of the same topological nature. Here, we demonstrate a robust photonic zero mode sustained by a spatial non-Hermitian phase transition in a parity-time (PT) symmetric lattice, despite the same topological order across the entire system. The non-Hermitian-enhanced topological protection ensures the re-emergence of the zero mode at the phase transition interface when the two semi-lattices under different PT phases are decoupled effectively in their real spectra. Residing at the mid-gap level of the PT symmetric spectrum, the zero mode is topologically protected against topological disorder.

The design of the zero mode is based on a non-Hermitian extension of the Su-Schrieffer-Heeger (SSH) model, where the tight-binding sites are modulated with alternating losses to construct a passive PT system, which has similar PT phase transition in a gain/loss balanced system. We realize a quantum phase transition interface (i.e. from PT symmetric phase to PT broken phase) between two semi-infinite lattices with a uniform topological order, as shown in **Fig. 5a**. Due to the lack of paired state from the left lattice to compensate the energy splitting in the right lattice, the edge state in the right lattice emerges as a localized zero mode at the interface site, as shown in the left panel of **Fig. 5b**. Recovered by the enhanced non-Hermiticity in the PT-broken lattice, the zero mode appears as a topologically isolated state and acquires protection against perturbation. The right panel in **Fig. 5b** shows the robustness of the zero mode against random perturbations of the coupling strengths at the interface site. Due to the similarities between the time-dependent Schrödinger equation and the paraxial wave functions, the tight-bind model can be approximated by a coupled waveguide array, in which the coupling strengths are defined by the spacing between adjacent waveguides. The onsite loss contrasts are effectively determined by the different amount of metal deposition on the top of the waveguide. As a result, a robust photonic zero mode with strong field localization emerges at the interface waveguide, shown in the background of **Fig. 5c**.

To reveal the zero-energy characteristics of the interface state, a control study was performed on the interface waveguide array together with a single waveguide as the reference by the heterodyne ultrafast measurements. The field images were reconstructed in **Fig. 6a** under same wave packet excitation to characterize the pulse propagation in the waveguide array (top panels) and the reference waveguide (bottom panels). **Fig. 6b** tracks the centers of the wave packets travelling in time for both the interface state and the single waveguide mode, which indicates the same propagation speed of the wave packets. The measured group index for the interface state is approximately $n_g = 3.97$, corresponding to an effective phase index of $n_{eff} = 2.37$ at 1550nm, which are almost identical to the group and phase indices of the single waveguide of approximately $n_g = 3.97$ and $n_{eff} = 2.37$, respectively, evidently showing the zero-energy properties.

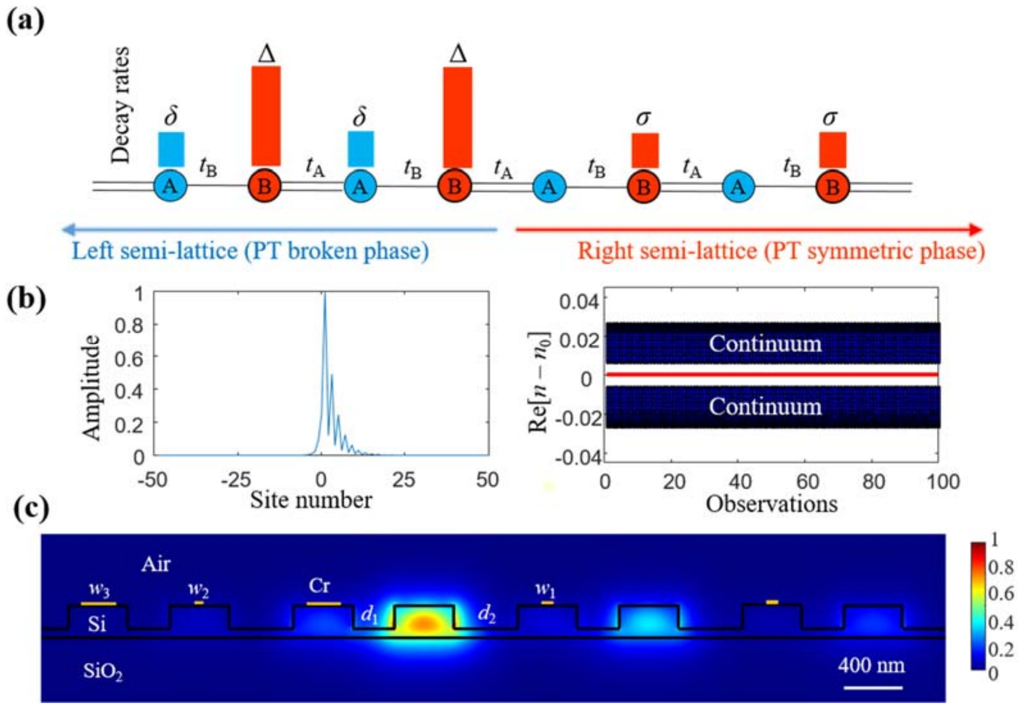

Figure 5. Implementation of the photonic zero mode. (a) Schematic of an interface formed by two different loss contrast over a uniform topology-ordered lattice. (b) Eigenvalue analysis of the system: amplitude distribution of the zero-energy interface state (left panel), and the robustness of the zero mode (red line) under random perturbations to the coupling strengths at the interface site. (c) Normalized electric field distribution of the photonic zero mode in a coupled waveguide array. The coupling strength and the onsite loss are defined by waveguide spacing distance and amount of Chromium (Cr) deposition respectively.

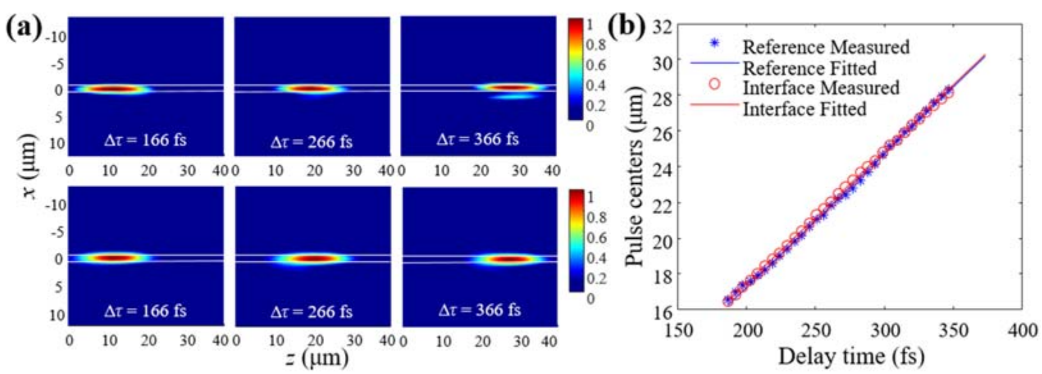

Figure 6. Ultrafast measurements of the photonic zero mode. (a) Reconstructed electric field images at 166fs, 266fs, and 366fs of the photonic zero mode (top panels) and the reference single waveguide (bottom panels) under the same excitation. (b) Heterodyne measurement results clearly show the zero-energy propagation the zero mode.

To test the robustness of the zero mode, the local topological perturbation is intentionally introduced to the interface waveguide, as shown in **Fig. 7a**. The interface waveguide is shifted by 100 nm towards the adjacent dimer in the PT symmetric semi-lattice. In this case, therefore, the local topological order is reversed. To enable the adiabatic transition between two opposite local topological orders, the shift of the interface waveguide gradually completes over a distance of 5 μm in the z direction. The zoom-in picture of the sample clearly confirms the implementation of this topology-transition region along the interface waveguide (**Fig. 7b**). Here, we performed both numerical simulations (**Fig. 7c**) and heterodyne measurements (**Fig. 7d**) to characterize a wave packet propagation supported by the zero mode, showing the pulse entering, propagating, and exiting around the topology-transition region. With the same single-waveguide excitation launched at the interface, the original zero mode is well formed in the interface waveguide. While the local topology varies after the wave packet enters the transition region, the zero mode persists with strong light localization at the interface. It is clear that the shape and dispersion of the wave packet after exiting the transition region remain almost unaffected, indicating the robust light transport carried by the zero mode. This is because the zero mode is protected under the PT symmetry invariants, even though the local topological order is completely reversed. The quantitative evaluation in experiments further confirms the robustness of the zero mode: the average group and phase indices during the topology transition are approximately $n_g = 3.97$ and $n_{eff} = 2.37$, which are almost identical to their counterparts of the zero mode without any disorder and perturbation.

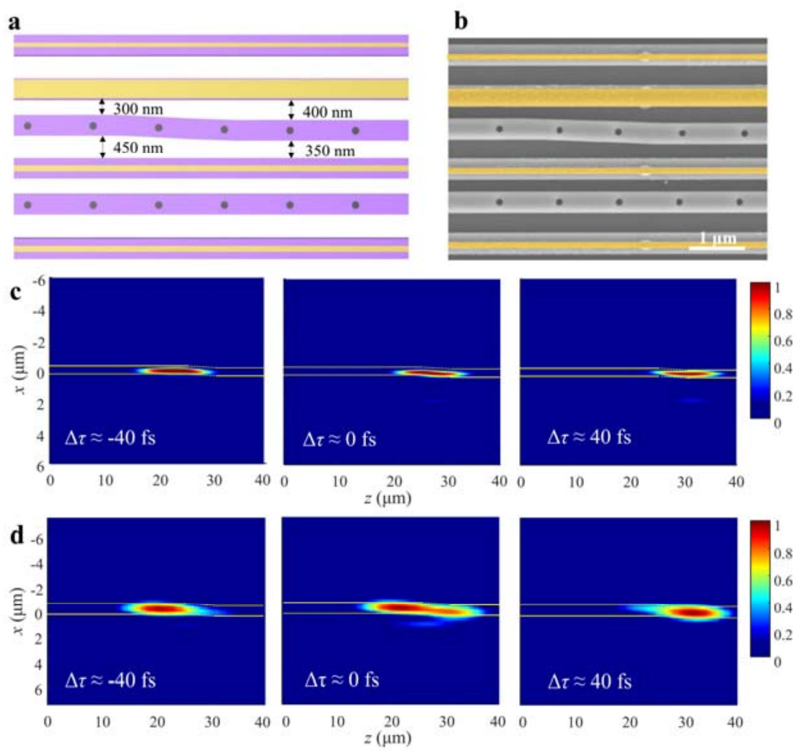

Figure 7. Experimental validation of the robustness of the zero mode. (a) The interface waveguide is adiabatically shifted 100 nm towards the PT symmetric semi-lattice over a distance of 5 μm in the z direction, reversing the local topological order around the interface from $t_A / t_B = 2.5$ to $t'_A / t'_B = 0.8$. (b) SEM picture of the topology-transition region implemented in the Si waveguide array, where pseudo yellow color denotes the Cr depositions. (c) and (d) are numerically simulated (c) and experimentally (d) measured ultrafast dynamics of the zero mode to probe its robustness against topological disorders. Snapshots at different time delays show the pulse entering, propagating, and exiting around the topology-transition region.

In summary, we have demonstrated experimentally a novel photonic zero mode spatially localized at the interface separating broken and unbroken PT phases. Through this non-Hermitian engineering, the interface state emerges as a dominant zero mode in the system of a uniform topological order. The restoration of topological protection of edge states in the lattice with a uniform topological order is enabled by the spatial quantum phase transition and enhanced by non-Hermitian loss engineering in the semi-lattices. Our strategic quantum phase manipulation thus provides a genuine new route toward the creation and manipulation of topological protected states in non-Hermitian photonics and beyond.

Non-Hermitian Modulated Topological Interface State Lasing

The discovery of topological band theory has ushered in a new era in condensed matter physics, providing intriguing insights into the world of low-dimensional quantum systems. Inspired by this groundbreaking work, topological mechanisms of optical mode formation have been proposed. The subsequent investigations of passive topological photonic systems have facilitated unidirectional transport channels. However, these pioneering studies have been limited in scope, exploring only a small subset of the full design parameter space. Active optical systems involving feedback mechanisms provide a much wider arena in which topological robustness collides with other physical considerations, posing diverse unexplored fundamental questions about the interplay between topological features and non-Hermitian physics. The answers to these questions transform our understanding of topological robustness by revealing unique connections between topology and other types of fundamental symmetries arising from non-Hermiticity. This new paradigm dictates a fresh look at the basic notion of topological protection in order to take into account the expanded design parameters space and establish a connection between topological physics and various separate activities on non-Hermitian photonic systems.

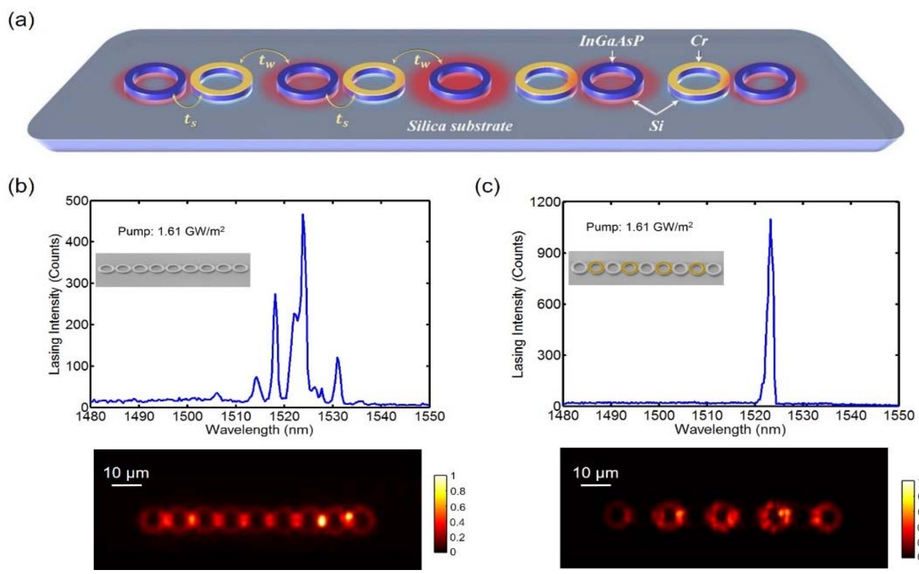

Figure 8. Non-Hermitian modulated zero state lasing. (a) Schematic of a topological laser array made of 9 microring resonators with alternating weak and strong couplings. A layer of 10-nm Cr (shown in yellow) is deposited on top of every second element to introduce distributed gain and loss. The red halos represent the intensity profile of the oscillating zero-mode. (b) Multimode lasing from an identically-sized microlaser array, but without on-top Cr deposition on every second ring to introduce the distributed gain/loss profile. (c) Single-supermode lasing from the topological microlaser with spatially distributed gain/loss. Emission spectra (top panels) and lasing mode profiles (lower panels) are measured for both laser arrays.

Here, we experimentally explore the utility of topological concepts to active systems and demonstrate an on-chip hybrid silicon microlaser whose mode competition naturally favors robust laser action arising from a topological defect. Our topological laser structure is an array of coupled InGaAsP-silicon microring resonators on a silicon-on-insulator (SOI) substrate (**Fig. 8a**), whose topological features arise from a sequence of alternating couplings precisely controlled by the separations between adjacent rings in an alternative fashion. A spacing defect in the center of the array creating a topological zero-mode that decays exponentially away from the defect, and only populates every other resonator. Spectrally, the topologically-protected zero-mode resides at the center of a band gap, where the symmetric features of the passive band structure arise from a chiral symmetry—a symmetry which maps the two symmetric bands onto each other. This symmetry is specifically related to inverting the sign of the couplings, which forces the zero-mode onto one "bright" sublattice. The distributed gain and loss respect a non-Hermitian charge-conjugation symmetry, leading to a response that robustly discriminates between the topological and non-topological states. In the complex frequency plane, this directly translates into an enhanced gain of the topological zero-mode state, therefore favoring it over other states throughout the nonlinear mode competition process.

In our experiment, we intentionally design a large-area single-mode laser with the transverse dimension of the hybrid ring being 1 μm wide and 720 nm thick (500 nm InGaAsP and 220 nm silicon). In this regard, while each ring supports several transverse modes, the fundamental transverse mode selected for the zero-mode occupies a much larger area of gain compared with the array of single-transverse-mode rings. In order to confirm the role of topological features in the mode selection process, a control experiment was conducted using an identically-sized microlaser array without the designed distributed gain/loss profile. As expected, the hybridization through couplings of all the transverse and longitudinal modes under the uniform pumping scenario displays a broader emission spectrum with multiple peaks and a reduced peak intensity, with the total emission homogeneously distributed over the entire structure (**Fig. 8b**). In contrast, the zero-mode lasing in the topological array is highly reliable, despite the mode competition in each ring and across rings (**Fig. 8c**), which is a direct outcome of the interplay between the topological mode hybridization and non-Hermiticity.

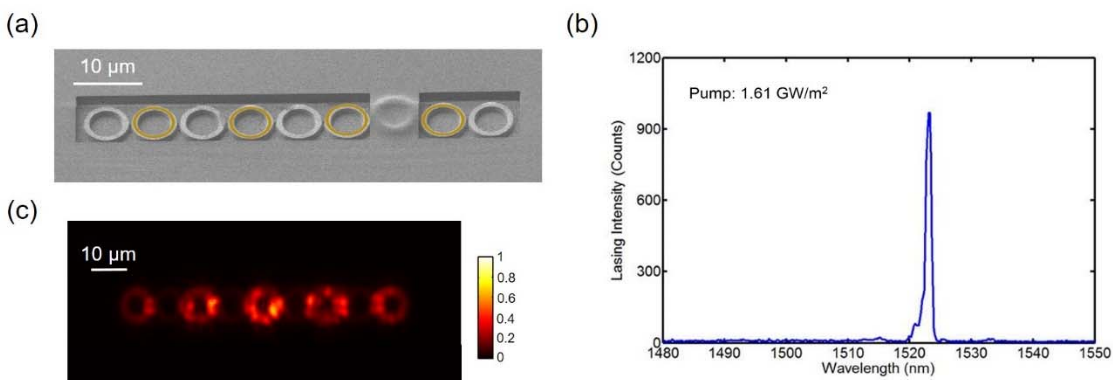

Figure 9. Robust zero mode laser action. (a) SEM of the perturbed topological laser array by depositing a thick layer of polymer covering the corresponding ring. (b) Measured emission spectrum of single-mode lasing from the perturbed laser array. (c) Measured intensity profile featuring the robustness of the topologically-protected zero-mode lasing against the introduced onsite perturbation.

One of the most important features of topological states is their robustness against defects and disorders. In particular, the spectral features of the zero-mode are known to be insensitive to off-diagonal perturbations represented by the coupling coefficients. Moreover, we find that the active system can still display a certain level of immunity against diagonal perturbations. In other words, the zero-mode lasing can well survive with onsite perturbations despite a slight spectral shift of the mode energy. To confirm this prediction experimentally, we introduced a polymer layer on top of the third ring resonator from the right to introduce a shift in its resonant frequency (**Fig. 9a**) and measured the emission spectrum (**Fig. 9b**). It is evident that the zero-mode lasing still persists with a high extinction ratio, without appreciable change in the spatial emission profile (**Fig. 9c**) apart from very small intensities leaking to the otherwise dark sublattice.

In summary, we have presented the demonstration of a topologically robust single-mode hybrid silicon microlaser. The interplay between topology and non-Hermitian symmetries equips the emerging topological zero-mode with a distinct mode profile that enables it to fully exploit the distributed gain domains, while simultaneously spoiling other states through deliberately introduced optical absorption. The demonstrated laser action is stable and immune to moderate perturbations since the zero-mode is topologically protected by the applied symmetries. Realized in a hybrid III-V/silicon platform, our accomplished topological hybrid silicon microlaser supports large-area single-supermode operation, promising a highly-efficient optical source for integrated silicon photonics to robustly feed power for chip-scale communication and computing.